NUMERICAL ANALYSIS OF MECHANICS OF HIGHLY EXTENSIBLE CABLES

Liércio André Isoldi
Ocean Engineering – FURG
liercioisoldi@bol.com.br

Maria Angela Vaz dos Santos
Ocean Engineering – FURG
angela@dmc.furg.br

Abstract. *The mechanics of highly extensible cables must be studied by numerical methods. For that reason, the computational implementation of a system of equations, which is capable to describe the motion of extensible cables, was developed. A local and a global system of reference were employed. Euler parameters represent the relative rotation between these systems of coordinates, avoiding the singularity associated to the Euler angles were used. It is necessary to include bending-stiffness in the governing equations, because a null or negative value of the axial stress in some part of the cable is possible. An implicit finite difference scheme was used to obtain the numerical solution of governing equations. This numerical model was used to analyze the dynamic behavior of a synthetic cable during and after a rupture. It was observed that the initial static tension of the cable is a decisive factor and when rupture takes a long time to occur a better dissipation of energy along the cable takes place. Hence, this cable is less destructive than a cable breaking quickly.*

Keywords. *highly extensible cables, dynamic analysis, finite difference, numerical simulation.*

1. Introduction

Synthetic cables have significant advantages for certain applications over metallic cables, because they are considerably lighter and can absorb imposed dynamic motions through extension without causing excessive dynamic tension. Extensible synthetic cables are characterized by a significantly smaller value of Young's modulus, compared with metallic cables, and hence, large extensibility under normal operating conditions. Whereas the maximum strain in a metallic cable under breaking tension is of the order of 2%, some synthetic cables reach or exceed a maximum strain of 25% (Triantafyllou e Yue 1995). The small value of Young's modulus affects both their bending properties and their elastic behavior. The bending stiffness of synthetic cables is two to three orders of magnitude lower than steel cables having the same strength (Tjavaras, 1996).

Synthetic ropes have a non-linear stress-strain relation. This non-linearity causes the speed of propagation to vary along the cable, since the tension, in general, varies along the cable (Tjavaras, 1996).

This paper presents a numerical simulation used to analyze the dynamic behavior of a highly extensible cable during and after a rupture.

2. Mathematic formulation

According to Tjavaras (1996) to derive the equations of motion, we assume that: the cross-section of the cable is homogeneous and circular or annular; the Euler-Bernoulli beam model represents adequately the effects of bending; and the tension is a single-valued function of the strain (Tjavaras et al., 1998).

We define two coordinate systems: (X, Y, Z) is a space-fixed rectangular coordinate system with unit vectors $\vec{i}, \vec{j}$ and $\vec{k}$; (x, y, z) is a local, Lagrangian reference frame with unit vectors $\vec{t}, \vec{n}$ and $\vec{b}$, where $\vec{t}$ points in the direction of the local tangent of cable, $\vec{n}$ in the direction of the maximum curvature, and $\vec{b}$ in the bi-normal direction.

The unit vectors of the local reference frame can be written as linear combinations of the unit vectors of the fixed reference frame:

$$\begin{bmatrix} \vec{t} \\ \vec{n} \\ \vec{b} \end{bmatrix} = [C] \begin{bmatrix} \vec{i} \\ \vec{j} \\ \vec{k} \end{bmatrix}. \tag{1}$$

The matrix $[C]$ is called the rotation matrix, because it describes the rotation matrix from the fixed to the local reference frame (Tjavaras, 1996).

An alternative method of describing the rotation form fixed to Lagrangian frames is the method using Euler parameters, which shows no singularity. The method was first used in cables by Hover (1997), and is based on the *principal rotation theorem* derived by Euler: an arbitrary orientation change can be achieved by a single rotation

through a principal angle α about a principal unit vector $\bar{1}$. The four Euler parameters are defined in terms of α and components of $\bar{1}$:

$$\vec{\beta} = \begin{bmatrix} \beta_0 \\ \beta_1 \\ \beta_2 \\ \beta_3 \end{bmatrix} = \begin{bmatrix} \cos(\alpha/2) \\ 1_x \, \text{sen}(\alpha/2) \\ 1_y \, \text{sen}(\alpha/2) \\ 1_z \, \text{sen}(\alpha/2) \end{bmatrix} \tag{2}$$

in terms of which, the rotation matrix can be in the form:

$$[C] = \begin{bmatrix} \beta_0^2 + \beta_1^2 - \beta_2^2 - \beta_3^2 & 2(\beta_1\beta_2 + \beta_0\beta_3) & 2(\beta_1\beta_3 - \beta_0\beta_2) \\ 2(\beta_1\beta_2 - \beta_0\beta_3) & \beta_0^2 - \beta_1^2 + \beta_2^2 - \beta_3^2 & 2(\beta_2\beta_3 + \beta_0\beta_1) \\ 2(\beta_1\beta_3 + \beta_0\beta_2) & 2(\beta_2\beta_3 - \beta_0\beta_1) & \beta_0^2 - \beta_1^2 - \beta_2^2 + \beta_3^2 \end{bmatrix}. \tag{3}$$

Considering an arbitrary vector $\vec{G} = \vec{G}(s,t)$, $\vec{G} = [G_x, G_y, G_z]$ in the fixed reference frame. Going to the local reference frame, $\vec{G} = [G_1, G_2, G_3]$. These two expressions of $\vec{G}$ are linked by the rotation matrix

$$\begin{bmatrix} G_1 \\ G_2 \\ G_3 \end{bmatrix} = [C] \begin{bmatrix} G_x \\ G_y \\ G_z \end{bmatrix}. \tag{4}$$

We denote the angular velocity of the local reference frame with respect to the fixed reference frame by $\omega(s,t)$ and the Darboux vector of the cable by $\Omega(s,t)$, then the derivatives of $\vec{G}$ are given by:

$$\frac{D\vec{G}}{Dt} = \frac{\partial \vec{G}}{\partial t} + \vec{\omega} \times \vec{G} \tag{5}$$

e

$$\frac{D\vec{G}}{Ds} = \frac{\partial \vec{G}}{\partial s} + \vec{\Omega} \times \vec{G}. \tag{6}$$

2.1. Balance of forces

Consider an infinitesimal segment of the cable of unstretched length ds centered at the point s, as shown in Fig. (1). Under the applied internal and external forces and moments, the segment ds stretches to a length ds_1.
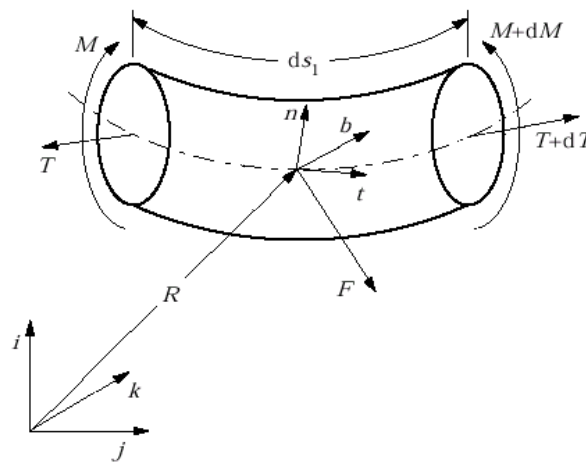

Figure 1. Cable segment.

The position of this point s at any time t is given by the vector $R(s,t)$, and the velocity vector is given by

$$\vec{V} = \frac{\partial \vec{R}}{\partial t} = u\vec{t} + v\vec{n} + w\vec{b} = U\vec{i} + V\vec{j} + W\vec{k}. \tag{7}$$

The strain $\varepsilon(s,t)$ at the point s is defined as

$$\varepsilon = \frac{ds_1 - ds}{ds}. \tag{8}$$

The vector $\vec{t}(s,t)$ tangent to the center-line of the cable is defined as

$$\vec{t} = \frac{\partial \vec{R}}{\partial s_1}. \tag{9}$$

For synthetic cables the Poisson ratio is $\nu = 0,5,$ and the volume of the cable segment is conserved. Then

$$A_1 = A\frac{ds}{ds_1} = A\frac{1}{1+\varepsilon}, \tag{10}$$

where A and A_1 are the cross-sectional areas before and after stretching.

Let m denote the mass per unit unstretched length of the cable and m_1 denote the mass per unit stretched length, the principle of conservation of mass applied to the segment ds of the cable gives

$$m_1 = m\frac{ds}{ds_1} = m\frac{1}{1+\varepsilon}. \tag{11}$$

Thus with the internal force vector $\vec{T} = T\vec{t} + S_n\vec{n} + S_b\vec{b},$ applying Newton's second law and considering the Eq. (5), (6), (8) and (11) we get

$$m\left(\frac{\partial \vec{V}}{\partial t} + \vec{\omega} \times \vec{V}\right) = \frac{\partial \vec{T}}{\partial s} + \Omega \times \vec{T} + (1+\varepsilon)\vec{F}, \tag{12}$$

where T, S_n and S_b denote the tangential, normal and binormal components of the internal force; $\vec{F}$ denotes the total external forces per unit length applied to the cable segment; and $(1+\varepsilon)\vec{F} = -w_0\vec{i}$, where w_0 is the weight of the cable.

2.2. Balance of moments

Considering the Fig. (1) the internal moment vector is given by

$$\vec{M} = M_t\vec{t} + M_n\vec{n} + M_b\vec{b}, \tag{13}$$

where $M_t = GI_p\Omega_1$ is a torsional component and $M_n = EI\Omega_2$ and $M_b = EI\Omega_3$ are the bending components, with EI representing the bending stiffness and GI_p the torsional stiffness of the cable.

So the balance of moments equation is given by:

$$\frac{1}{(1+\varepsilon)^2}\frac{\partial \vec{M}}{\partial s} + \frac{1}{(1+\varepsilon)^2}\vec{\Omega} \times \vec{M} + (1+\varepsilon)\vec{t} \times \vec{T} = 0. \tag{14}$$

2.3. Compatibility relations

For the configuration of the cable to be continuous we must enforce the compatibility relation. The vector $\vec{R}$ and its partial derivatives are continuous in t and s, so:

$$\frac{\partial \varepsilon}{\partial t}\vec{t} + (1+\varepsilon)\vec{\omega} \times \vec{t} = \frac{\partial \vec{V}}{\partial s} + \vec{\Omega} \times \vec{V}. \tag{15}$$

2.4. Space derivatives of Euler parameters

According to Hover (1997) we will use the equations that define the space derivatives of the Euler parameters in terms of the cable's curvature thus

$$\frac{\partial\vec{\beta}}{\partial s} = \frac{1}{2}\begin{bmatrix} \beta_0 & -\beta_1 & -\beta_2 & -\beta_3 \\ \beta_1 & \beta_0 & -\beta_3 & \beta_2 \\ \beta_2 & \beta_3 & \beta_0 & -\beta_1 \\ \beta_3 & -\beta_2 & \beta_1 & \beta_0 \end{bmatrix}\begin{Bmatrix} 0 \\ \vec{\Omega} \end{Bmatrix}. \tag{16}$$

2.5. Tension-strain relation

As in Tjavaras et al. (1998), for a nylon double braid line, the tension T and the strain ε at any point along the cable are related by

$$T = f(\varepsilon) = p_1 \tanh(p_2\varepsilon + p_3) + p_4 + p_5\varepsilon, \tag{17}$$

where $p_1 = 2{,}703 \times 10^5$ N, $p_2 = 10{,}2$, $p_3 = -2{,}128$, $p_4 = 2{,}627 \times 10^5$ N and $p_5 = 135{,}5$ N.

2.6. Equations of motions

The vector form of the equations of motion is given by

$$\frac{\partial\vec{Y}}{\partial s} + [M](\vec{Y})\frac{\partial\vec{Y}}{\partial t} + \vec{P}(\vec{Y}) = 0. \tag{18}$$

However we will study a bi-dimensional case thus the vector $\vec{Y}$ assumes the form

$$\vec{Y} = \begin{bmatrix} \varepsilon & S_n & u & v & \beta_0 & \beta_3 & \Omega_3 \end{bmatrix}^T, \tag{19}$$

and the matrix $[M]$ and the vector $\vec{P}$ are defined respectively as

$$[M(\vec{Y})] = \begin{bmatrix} 0 & 0 & -\dfrac{m}{f'(\varepsilon)} & 0 & -\dfrac{2m(v\beta_3)}{f'(\varepsilon)} & \dfrac{2m(v\beta_0)}{f'(\varepsilon)} & 0 \\ 0 & 0 & 0 & -m & 2m(u\beta_3) & -2m(u\beta_0) & 0 \\ -1 & 0 & 0 & 0 & 0 & 0 & 0 \\ 0 & 0 & 0 & 0 & 2(1+\varepsilon)\beta_3 & -2(1+\varepsilon)\beta_0 & 0 \\ 0 & 0 & 0 & 0 & 0 & 0 & 0 \\ 0 & 0 & 0 & 0 & 0 & 0 & 0 \\ 0 & 0 & 0 & 0 & 0 & 0 & 0 \end{bmatrix} \tag{20}$$

$$\vec{P}(\vec{Y}) = \begin{bmatrix} -\dfrac{S_n\Omega_3}{f'(\varepsilon)} - \dfrac{w_0}{f'(\varepsilon)}\left(\beta_0^2 - \beta_3^2\right) \\ f(\varepsilon)\Omega_3 + 2w_0(\beta_0\beta_3) \\ -\Omega_3 v \\ \Omega_3 u \\ \dfrac{1}{2}(\beta_3\Omega_3) \\ -\dfrac{1}{2}(\beta_0\Omega_3) \\ \dfrac{1}{EI}S_n(1+\varepsilon)^3 \end{bmatrix}. \tag{21}$$

3. Numerical method

According to Tjavaras et al. (1998) a finite-difference scheme, called box method, is employed to solve the Eq. (18). With this method, the implicit scheme is used for time integration.

The cable is divided into $n_p - 1$ discrete segments of unstretched length $\Delta s_{(k)}$ by means of n_p points numbered $(k = 1, 2, ..., n_p)$. The length of the segments is not necessarily constant along the cable. We define the discrete segment length $\Delta s_{(k)}$ as the length of the segment between the computational points k and $k+1$.

At each moment in time t_i we know the values of the unknown variables $Y_{i-1,k}$ at all points on the cable at the previous time step $t_{i-1} = t_i - \Delta t$, where Δt is the computational time step. We need to calculate the values of the unknown variables at the present time. To do so we write the discrete form of the system of governing equations in the mid-point $\left(k - \frac{1}{2}, i - \frac{1}{2}\right)$ of each computational "box". The values of each variable are approximated by

$$\vec{Y}_{k-\frac{1}{2}, i-\frac{1}{2}} \rightarrow \frac{1}{4}\left(\vec{Y}_{k-1,i-1} + \vec{Y}_{k-1,i} + \vec{Y}_{k,i-1} + \vec{Y}_{k,i}\right) \tag{22}$$

The time and space derivatives of the dependent variables are written as

$$\left(\frac{\partial \vec{Y}}{\partial t}\right)_{k-\frac{1}{2}, i-\frac{1}{2}} \rightarrow \frac{1}{2}\left(\frac{\vec{Y}_{k-1,i} - \vec{Y}_{k-1,i-1}}{\Delta t} + \frac{\vec{Y}_{k,i} - \vec{Y}_{k,i-1}}{\Delta t}\right), \tag{23}$$

$$\left(\frac{\partial \vec{Y}}{\partial s}\right)_{k-\frac{1}{2}, i-\frac{1}{2}} \rightarrow \frac{1}{2}\left(\frac{\vec{Y}_{k,i-1} - \vec{Y}_{k-1,i-1}}{\Delta s_{(k-1)}} + \frac{\vec{Y}_{k,i} - \vec{Y}_{k-1,i}}{\Delta s_{(k-1)}}\right). \tag{24}$$

Using the Eq. (22), (23) and (24) we can write the discrete approximation of the system of partial differential equations that govern the motion of cable at the point $\left(k - \frac{1}{2}, i - \frac{1}{2}\right)$

$$2\Delta t\left(\vec{Y}_{k,i} - \vec{Y}_{k-1,i} + \vec{Y}_{k,i-1} - \vec{Y}_{k-1,i-1}\right) +$$
$$\Delta s_{(k)}\left[\left(\left[M_{k-1,i}\right] + \left[M_{k-1,i-1}\right]\right)\left(\vec{Y}_{k-1,i} - \vec{Y}_{k-1,i-1}\right) + \left(\left[M_{k,i}\right] + \left[M_{k,i-1}\right]\right)\left(\vec{Y}_{k,i} - \vec{Y}_{k,i-1}\right)\right] +$$
$$\Delta t \Delta s_{(k)}\left(\vec{P}_{k-1,i-1} + \vec{P}_{k-1,i} + \vec{P}_{k,i-1} + \vec{P}_{k,i}\right) = 0. \tag{25}$$

Thus for each mid-point $\left(k - \frac{1}{2}, i - \frac{1}{2}\right)$ we have a system of n_e equations. $n_e = 7$ is the number of equations in the system of the Eq. (18) and also the size of the vector $\vec{Y}$ of the dependent variables. These n_e equations involve the dependent variables at two neighboring points $k-1$ and k. By writing the Eq. (25) for all points $\left(k - \frac{1}{2}, i - \frac{1}{2}\right)$, $k = 2, 3, ..., n_p$, we end up with a system of $n_e \cdot (n_p - 1)$ equations in $n_e \cdot n_p$ unknowns $\vec{Y}_{k,i}$, $k = 1, 2, ..., n_p$. The n_e equations necessary to make the system solvable are provided by the boundary conditions at the points $k = 1$ and $k = n_p$, and are given respectively by

$$\begin{cases} u = 0; \\ v = 0; \\ \dfrac{\partial \Omega_3}{\partial t} = 0. \end{cases} \tag{26}$$

and

$$\begin{cases} f(\varepsilon) \geq T \geq 0 \text{ for time} < t_{br} \text{ or } T = 0 \text{ for time} > t_{br} \\ S_{n\,est.} \geq S_n \geq 0 \text{ for time} < t_{br} \text{ or } S_n = 0 \text{ for time} > t_{br} \\ \dfrac{\partial \Omega_3}{\partial t} = 0 \\ \beta_0^2 + \beta_3^2 = 1 \end{cases} \tag{27}$$

where t_{br} is the breaking time.

In order to solve the system of equations for the dependent variables was necessary to calculate analytically the Jacobian of the system, obtaining an efficient numeric code, that was solved by the LU decomposition with pivoting, as shown in Isoldi (2002).

The initial condition for the solution of the dynamic analysis is the solution of the static analysis. And the initial condition of the static analysis is the catenary of cable. The system of equations for the static analysis can be easily obtained, considering in the Eq. (18) the speed of the cable and whole derived them in the time as null.

The boundary conditions for the static analyses at the points $k = 1$ and $k = n_p$ are given respectively by

$$\begin{cases} S_n = 0 \\ T = f(\varepsilon) = \text{cte.} \end{cases} \tag{28}$$

and

$$\begin{cases} S_n = 0 \\ T = f(\varepsilon) = \text{cte.} \\ \beta_0^2 + \beta_3^2 = 1 \end{cases} \tag{29}$$

4. Post-rupture behaviour of a synthetic cable

Synthetic cables stretch up to thirty times more than steel cables before reaching their breaking strength. Thus they can store a larger amount of potential energy, which is suddenly transformed into kinetic energy when the cable breaks (Tjavaras, 1996).

4.1 Problem definition

Consider a 60 m long synthetic cable whose end-points are held fixed at the same vertical level. The catenary shape of the cable will lie in the vertical plane containing its two end-points. The dimensions and physical properties of the cable are

unstretched length	$\rightarrow \ell = 60\,\text{m}$;
diameter	$\rightarrow d = 0{,}05\,\text{m}$;
cross-sectional area	$\rightarrow A = 1{,}964 \times 10^{-3}\,\text{m}^2$;
density	$\rightarrow \rho = 1140\,\text{kg}/\text{m}^3$;
Young's modulus	$\rightarrow E = 230\,\text{MPa}$;
Poisson ratio	$\rightarrow \nu = 0{,}5$.

The typical Young's modulus was calculated by:

$$E = \frac{T}{A\varepsilon}, \tag{30}$$

where $T = 45000\,\text{N}$ and $\varepsilon = 9{,}9\%$.

According to Tjavaras (1996) the cable is held at its initial position by horizontal and vertical forces applied at the end-points, and we assume that at the time $t = 0$ the cable breaks at one the end-points. In order to simulate the rupture, the horizontal and vertical external forces acting at the right end are quickly but smoothly reduced to zero. The horizontal force F_h and the vertical force F_v both reach zero at the breaking time $t = t_{br}$. Their variation with time is given by

$$F_h = F_{h,s} \cos^2\left(\frac{\pi}{2}\frac{t}{t_{br}}\right) \tag{31}$$

and

$$F_v = F_{v,s} \cos^2\left(\frac{\pi}{2}\frac{t}{t_{br}}\right), \tag{32}$$

where $F_{h,s}$ and $F_{v,s}$ are the static horizontal and vertical forces at the end of the cable, respectively.

4.2. Numerical simulations

We employ two different breaking times, called respectively fast rupture and slowly rupture. We used two values for initial static tension. These values are: (a) 180000 N producing a strain of 17,8% and (b) 315000 N producing a static strain of 22,8%.

For the fast rupture the breaking time is chosen to be $t_{br} = 5\,ms$. Figure (2) is a plot of the x-z motion of the breaking line. The line shows the successive configurations of the line at 10 ms apart. The total time for the simulation (a) is 0,14 s and for (b) is 0,13 s.
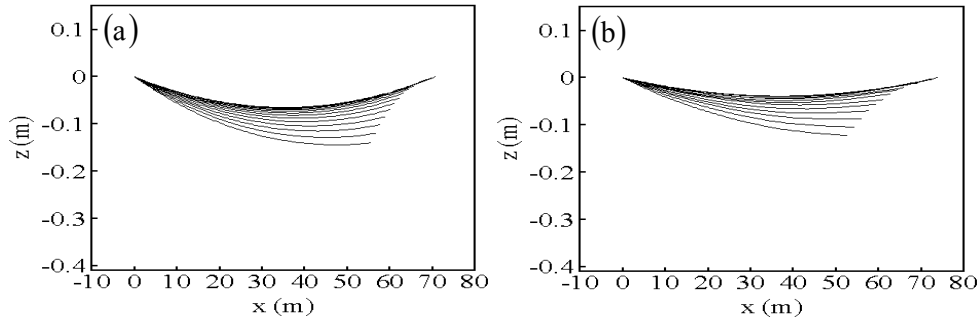
Figure 2. Motion of a breaking cable $(t_{br} = 5\,ms)$: (a) T=180000N and (b) T=315000N.

Notice that Fig. (2) is not drawn to scale: the vertical displacements are exaggerated by a factor of a hundred relative to the horizontal displacements. That is, while the recoil motion of the cable is of the order of meters, the vertical motion of the line, in the short time immediately after rupture, is of the order of centimetres.

The Fig. (3) shows the variation of the tension-distribution along the line with time and the Fig. (4) shows the variation with time of the velocity of each point of the cable.
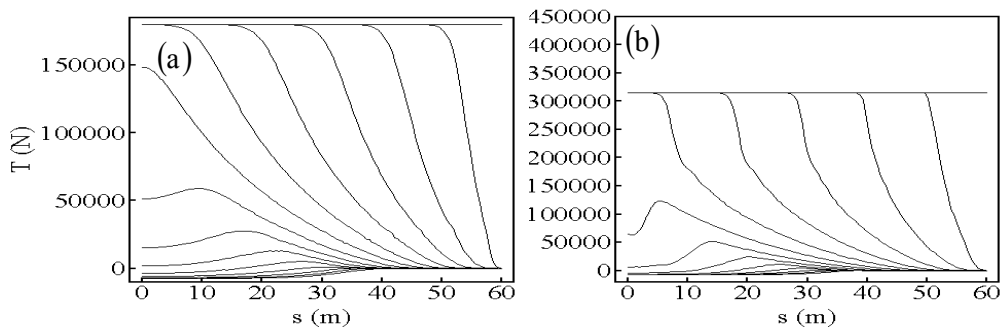

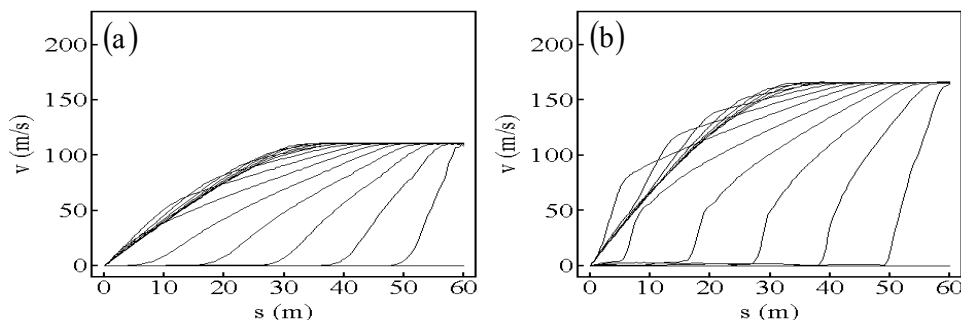Figure (3). Variation of the tension of a breaking cable $(t_{br} = 5\,ms)$: (a) T=180000N and (b) T=315000N.

Figure (4). Variation of the velocity of a breaking cable $(t_{br} = 5\,ms)$: (a) T=180000N and (b) T=315000N.

We can observe in Fig. (2) that cables submitted to higher tension, when suffer a rupture, answer with a larger kinetic energy, due to a larger stored potential energy. The largest horizontal motion described by these proves this. We also noted that happens a decrease in the vertical motion of the cable with the increase of the static tension.

In Fig. (3) the almost horizontal line at the top of each plot indicates the static tension for this run. The following lines show the tension dropping to zero at the right end and the front of "non-static" tension propagating towards the fixed end. The speed of propagation of this front is the speed of propagation of elastic waves and is given by:

$$c_{nl} = \sqrt{\frac{T'(\varepsilon)}{m}}, \tag{33}$$

and depends only the initial static tension.

We can also observe, in Fig. (2), that the compression in the left end of the cable, in Fig. (3), is not enough to cause buckling in this end.

We can see in Fig. (4) the horizontal line indicates that the velocity is initially zero and the velocity of the end-point, which is the maximum velocity in each case, is higher when the initial static tension is higher. This explains the fact that more energy is stored in the lines that are more highly tensioned.

According to Tjavaras (1996) cables that break slowly are safer. By "slowly rupture" we mean that the value of the tension at the breaking point takes longer to reach zero. Cables have been designed so that its strands do not fail all at the same time but successively. Thus the intact strands continue to carry loads, which are smaller than the static tension on the line but larger to zero. In order to study the slowly rupture we performed two runs where the breaking time is $t_{br} = 50 \, ms$. We employ the same values to the initial static tension and the same scale to plot the results. The line shows the successive configurations of the line at 10 ms apart. The total time for case (a) is 0,17 s and for (b) is 0,16 s.

Figure (5) shows the post-fracture motion of the breaking line in the x-z plane. The variation with time of the tension along the cable can be observed in Fig. (6). Finally, Fig. (7) shows the velocity distribution along the cable.
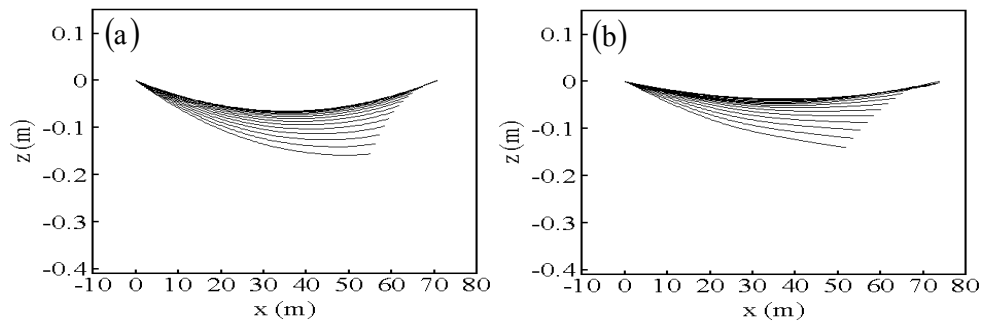

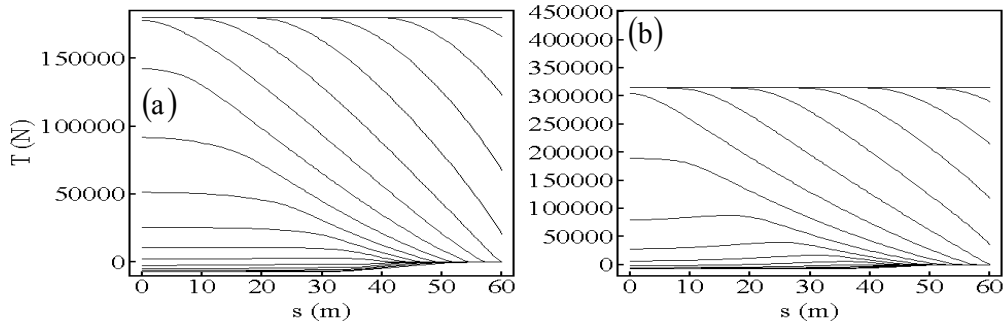Figure (5). Motion of a breaking cable $(t_{br} = 50 \, ms)$: (a) T=180000N and (b) T=315000N.

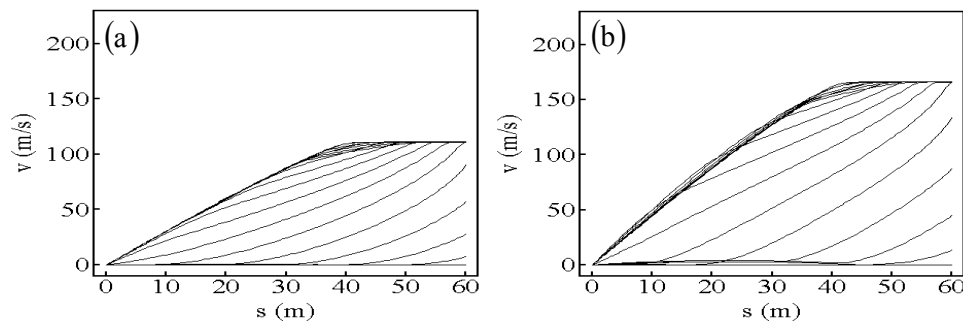Figure (6). Variation of the tension of a breaking cable $(t_{br} = 50 \, ms)$: (a) T=180000N and (b) T=315000N.

Figure (7). Variation of the velocity of a breaking cable $(t_{br} = 50 \, ms)$: (a) T=180000N and (b) T=315000N.

Comparing Fig. (5) with Fig. (2) we can observe that the motion of the cable is not significantly affected by the slower breaking time. The similarity in the motion between the fast-rupture and the slowly rupture runs hides differences that can be seen in the tension plots and the cable velocity plots.

We can see in Fig. (6) that the tension is more uniformly distributed along the cable. Indeed it takes longer for the tension at the breaking end to reach zero, therefore the variation in the tension is less abrupt. This has a noticeable effect on the velocity distribution. Hence, even though the total kinetic energy that must be dissipated after breaking depends only on the static tension and does not depend on the breaking time, the way the energy is dissipated does. Cables that are breaking more slowly dissipate the energy along a larger part of their length. Fast rupture cables have a portion of their length moving at maximum velocity and another part practically motionless, whereas slowly rupture cables have a larger part moving at moderate velocities and only a small region near the broken end moves at maximum speed. This is a possible explanation for the generally accepted view that slowly breaking cables are somewhat less destructive than fast breaking ones.

Here, as in the previous simulation, the compression in the left end is not enough to cause buckling.

Finally, in Fig. (7) we can see that the maximum velocity in the cable is not affected by the time it takes the cable to break. Only the static tension seems to affect the maximum velocity. On the other hand the time it takes for this maximum velocity to be reached varies. In the slowly breaking cases, it takes longer for the maximum velocity to be reached at the breaking end. Also, the length of the cable that moves with this maximum velocity is smaller in the slowly breaking runs. This implies that the kinetic energy is more uniformly distributed in the cable.

5. Conclusions

The ability of the cable model to simulate the post-rupture behavior of a synthetic cable was demonstrated. In simulations we can observe that the initial static tension affect the motion of the cable; the tension distribution along the cable; and the velocity of each point of the cable.

We can observe that the motion of the cable is not significantly affected by the different breaking times.

We find that in the slow rupture case, the tension distribution along the cable is more uniform, hence it takes longer for the tension at the breaking end to reach zero and therefore the variation in the tension is less abrupt. So cables that are breaking more slowly dissipate the energy along a larger part of their length, hence are less destructive than fast breaking ones.

Finally in the slowly breaking cases, it takes longer for the maximum velocity to be reached at the breaking end. The length of the cable that moves with this maximum velocity is smaller; hence the kinetic energy is more uniformly distributed along the synthetic cable.

6. Acknowledgement

7. References

Hover, F. S., 1997, "Simulation of stiff massless tethers", Ocean Engineering, Cambridge, Vol. 24,   No. 8, pp. 765-783.

Isoldi, L. A., 2002, "Análise numérica da dinâmica de cabos altamente extensíveis", Rio Grande, 143 f. Dissertation (Master in Ocean Engineering) – Ocean Engineering, FURG.

Tjavaras, A. A., 1996, "The dynamics of highly-extensible cables", Cambridge, 188 f. Thesis (Doctor of Philosophy) – Departament of Ocean Engineering, Massachusetts Institute of Technology.

Tjavaras, A. A. et al., 1998, "The mechanics of highly-extensible cables", Journal of Sound and Vibration, Vol. 213, No. 4, pp. 709-737

Triantafyllou, M. S., Yue, D. K. P., 1995, "Damping amplification in highly extensible hysteretic cables", Journal of Sound and Vibration, Vol. 186, No. 3, pp. 355-368.

8. Copyright Notice